On the reliability of low-pressure dc glow discharge modelling

Z Donkó[1], P Hartmann and K Kutasi

Research Institute for Solid State Physics and Optics of the Hungarian Academy of Sciences,
H-1525 Budapest, POB 49, Hungary

E-mail: donko@sunserv.kfki.hu

Abstract
Modelling approaches used for the description of the cathode region of dc
glow discharges are reviewed, with the focus on hybrid models which
combine the fluid description of positive ions and bulk electrons with the
kinetic simulation of fast electrons. The reliability of the calculated
discharge characteristics is analysed by testing the different assumptions of
the models and the sensitivity of the calculated characteristics on the input
data. The applicability of the particle-in-cell technique (complemented with
Monte Carlo simulation of collision processes) for the simulation of dc glow
discharges is also discussed.

1. Introduction

The cathode region of dc glow discharges is of interest both
from the point of view of applications (mostly due to the
presence of energetic particles) and also from the point of
view of theory (due to the complicated phenomenon of self-
sustainment influenced by numerous gas-phase and surface
processes and due to the non-equilibrium transport of charged
particles caused by the high spatial gradient of the electric field
near the cathode). In the last decade better understanding of
the operation of low-pressure glow discharges has been aided
by the development of comprehensive models, e.g. [1–11].

Uncertainties of modelling results originate mainly from
two principal sources. Part of the errors arise from the
simplification of the models (or the 'level' of the approach),
while the other part stems from the inaccuracy of the input data.

As far as the input data of the models are concerned, we
need to analyse the accuracy of the data characterizing gas
phase collisions and the transport of charged particles (cross
sections and transport parameters, like mobility and diffusion
coefficients), as well as those describing the interaction of
charged particles with electrode surfaces (the most important
being the secondary electron yield γ of the cathode).

The collision cross sections of electrons are relatively
well known, although data are less reliable for heavy-particle
collisions, as reviewed in [12]. Transport parameters used
in the models are usually taken from experimental studies,
which in most cases have an acceptable accuracy (in the
order of $\lesssim 10\%$). Since in dc discharges—unlike in the RF
case—charge reproduction at the electrode surface is always
important, the electron emission properties of the cathode
are of primary importance. The electron yields of cathode
materials, especially under gas discharge conditions, are
perhaps the least known data of gas discharge physics. At the
same time the results of modelling calculations sensitively
depend on the electron yield data. The issues associated with
the γ coefficients and their influence on the characteristics of
gas discharges began to receive renewed attention in the last
couple of years [13–22].

The modelling approaches can be categorized as (i) fluid
methods, (ii) (kinetic) particle methods and (iii) their
combinations, termed as hybrid methods. In this paper we
focus on hybrid methods representing a compromise between
the computationally very efficient fluid models (which, on
the other hand, have serious limitations) and fully kinetic
particle models that require very extensive computations (and
which may suffer from principal limitations in the case of
dc discharges). During the last decade hybrid models have
successfully been used in studies of numerous gas discharge
phenomena (e.g. calculations of apparent electron yield [16],
gas heating [23], transition from Townsend discharge to
abnormal glow [24], cathode sputtering [25], light emission
[26] and the hollow cathode effect [27]) and different *devices*
(e.g. pseudospark switches [2], plasma display panels [28],
discharge cells used for glow discharge spectroscopy [29] and
plasma thrusters [30]).

---

[1] Author to whom any correspondence should be addressed.

The hybrid approach has made it possible to gain a deep insight into the physics of these phenomena and the operation of these devices; however, some of the assumptions used in the models remained untested during the years. The main aim of the present work is to critically examine some of these assumptions. Section 2 of the paper describes the basics of fluid and hybrid models. Some representative results of these types of (one-dimensional (1D)) models are compared with each other and with experimental counterparts in section 3. The applicability of the particle-in-cell approach for the description of dc glow discharges is discussed in section 4. Section 5 presents the conclusions of the paper.

2. Fluid and hybrid models

The basic equations of fluid models are derived as velocity moments of the Boltzmann transport equation. In the simplest type of fluid models only the first two moments—expressing particle balance and momentum balance—are considered. The continuity equations and momentum transfer equations (which are usually written in the drift–diffusion approximation) for the electrons and ions are coupled with the Poisson equation in order to obtain a self-consistent solution (e.g. [2]):

$$\frac{\partial n_e}{\partial t} + \nabla(n_e v_e) = S_e - L_e, \tag{1}$$

$$\frac{\partial n_i}{\partial t} + \nabla(n_i v_i) = S_i - L_i, \tag{2}$$

$$\Phi_e = n_e v_e = -n_e \mu_e E - \nabla(n_e D_e), \tag{3}$$

$$\Phi_i = n_i v_i = n_i \mu_i E - \nabla(n_i D_i), \tag{4}$$

$$\triangle V = -\frac{e}{\epsilon_0}(n_i - n_e), \tag{5}$$

where n_e and n_i are the densities, Φ_e and Φ_i are the fluxes, v_e and v_i are the mean velocities, S_e and S_i are the source functions, μ_e and μ_i are the mobilities, D_e and D_i are the diffusion coefficients of electrons and ions, respectively, V is the electric potential, e is the elementary charge and ϵ_0 is the permittivity of free space. Additional charged species (like molecular ions appearing at elevated pressures [31–33], ions of the sputtered metal [34] or negative ions [35]) may as well be considered by complementing the above set with additional equations. The (gas-phase) losses L_e and L_i may show up due to processes like recombination, attachment, etc. The major contribution to the source terms S_e and S_i is usually due to electron impact ionization, but additional processes, e.g. ionization by heavy particles or metastable–metastable collisions, may also be important at certain conditions.

The above set of equations (1)–(5) is 'closed' by a number of boundary conditions, which usually assume zero density of charged particles and prescribed values of electric potential at the electrodes. The electron and the ion current densities at the cathode are related to each other through the apparent electron yield:

$$\gamma = \frac{j^-}{j^+}\bigg|_{\text{cathode}}. \tag{6}$$

In the case of the fluid (hydrodynamic) approach, moments of the distribution functions are assumed to depend exclusively on the *local* value of the reduced electric field E/n. In the simplest case when only electron impact ionization is

considered, the source terms of the continuity equations are calculated as

$$S_e(x) = S_i(x) = \alpha\left(\frac{E}{n}\right)\Phi_e(x), \tag{7}$$

where α is the first Townsend coefficient, which depends on the local value of the reduced electric field $E(x)/n$. Such a 'local-field' approach is expected to be sufficiently accurate as long as the electric field does not change significantly along the free path (λ) of particles, i.e.

$$\lambda\frac{dE}{dx} \ll E. \tag{8}$$

In hybrid models the electron impact contribution to S_i and the source term for slow electrons S_e are calculated at the kinetic level (which is valid for arbitrary values of the field gradient), from Monte Carlo simulation of the *fast* electrons (e.g. [2]). The fluid approach is still used for the positive ions and for the *slow* electrons, which are no longer able to excite or ionize the gas. The Monte Carlo module makes use of the electric field distribution obtained in the fluid module and provides the source functions of positive ions and slow electrons to be used in the continuity equations of the fluid module.

In an advanced class of hybrid models, the so-called 'heavy-particle hybrid models' (e.g. [36]), Monte Carlo simulation is also applied for the tracing of positive ions and fast neutral atoms in the cathode sheath. Fast neutral atoms originate from charge and momentum transfer collisions between positive ions and the atoms of the background gas, and—together with the positive ions—can contribute to a significant extent to (i) the electron emission at the cathode [37], (ii) the heating of the gas [16] and (iii) cathode sputtering [34]. Consequently in models which intend to include these effects, the kinetics of heavy particles has to be taken into account.

Regarding the transport coefficients which are needed as input data in the momentum balance equations (3) and (4), most of the hybrid modelling simulation studies published during the last decade have used the following assumptions. The mobility of positive ions μ_i is taken as a function of the reduced electric field E/n and their diffusion coefficient D_i is usually set to result $D_i/\mu_i = kT_g/e$ (where T_g is the gas temperature). This latter assumption—which implies that ions are thermalized through frequent collisions with background gas atoms—is acceptable in the negative glow, while in the cathode sheath their transport is predominantly determined by the drift in the strong electric field. Concerning the transport coefficients of electrons, for the mobility μ_e an experimental value at a low value of E/n is used in most of the works, and the E/n-dependence of μ_e is not considered. The diffusion coefficient of electrons D_e is in most cases chosen to result in a fixed $kT_e/e = D_e/\mu_e =$ const. characteristic energy for slow electrons. The value of kT_e usually fixed in the models to 1 eV (e.g. [2, 5, 38]) with very few exceptions (e.g. [31]) and this value is used as an *input* parameter in the hybrid models. The validity of this assumption remained obviously unquestioned in the numerous studies reported about hybrid simulations during the last decade, prior to our recent work [33]. It is noted that while in principle it would be possible to consider the full E/n-dependence of all the transport coefficients, in the case

of electrons this was found to give rise to numerical instabilities of the mathematical schemes routinely used in hybrid models.

An emerging possibility to overcome the above problems can be the use of the '*average energy approach*', in which the electron transport coefficients are functions of the local mean electron energy rather than the local value of the reduced electric field [39–42]. In this approach the simplified set of fluid equations (1)–(4) is complemented with an energy balance equation for the electrons, derived as the third velocity moment of the Boltzmann equation. Studies are currently underway to compare the fluid/hybrid modelling results presented in this paper with those obtainable from such an improved solution method.

3. Results and discussion

In the following, the effect of the secondary electron emission coefficient and the assumed value of the bulk electron temperature on the results calculated from hybrid models is investigated in detail. In parallel with this, the results of the hybrid models are compared with those of fluid models.

3.1. Effect of secondary yields

By defining the value of the γ coefficient as an input parameter of the model one can calculate the voltage–current characteristic of the discharge. The choice of γ is, however, far from being trivial, as different particles (positive ions, metastable atoms, fast neutrals as well as photons) contribute to the electron emission from the cathode, and their importance changes in a complex manner with the operating parameters and conditions [14, 16]. Moreover, as compared with clean environments (ion beam measurements on heavily sputtered samples under ultrahigh-vacuum conditions), cathode surfaces operated under discharge conditions can be characterized by fairly different secondary yield values [14, 22].

The effect of γ assumed in the model on the calculated voltage—current density curves of the helium discharge is illustrated in figure 1(*a*), for a pressure × electrode separation (pL) value of 3 Torr cm. The simulations based on a 1D hybrid model have been carried out using different values of the apparent secondary electron emission coefficient: $\gamma = 0.10$, 0.13, 0.16 and 0.3. The $\gamma = 0.3$ value corresponds to a clean metal surface, and it is close to the data obtained in measurements of electron yield due to He$^+$ bombardment, carried out under ultrahigh vacuum conditions and heavily sputtered samples. The $\gamma = 0.16$ value, on the other hand, is known to characterize gas covered copper cathodes [43]. The curves corresponding to these two different values of γ exhibit a pronounced difference. For comparison, an experimental curve—corresponding to $pL = 3.38$ Torr cm (obtained in an extensive experimental scan of the electrical characteristics of helium glow discharges) covering a wide range of pressure, electrode separation, current and voltage values [44]—is also plotted in figure 1(*a*). At the lower values of the reduced current density j/p^2 the experimental curve is near the one calculated at $\gamma = 0.16$, while at higher j/p^2 a somewhat lower value of γ results in a better agreement between the calculated and measured data. The discrepancy at higher j/p^2 values between
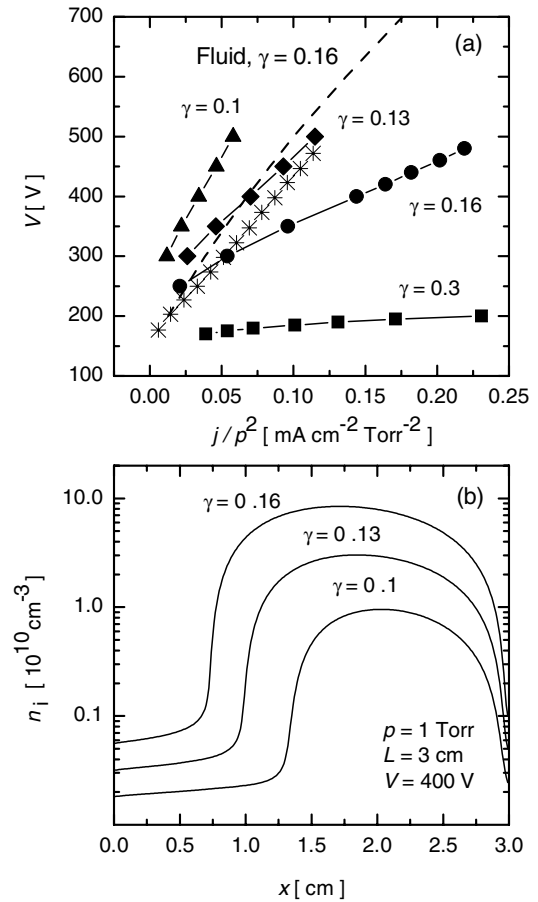

Figure 1. (*a*) Electrical characteristics of helium glow discharges. The 1D hybrid modelling results (filled symbols) obtained for $pL = 3$ Torr cm are shown for apparent secondary electron yield values $\gamma = 0.1$, 0.13, 0.16 and 0.3. $kT_e = 0.3$ eV is assumed in the model. The dashed line is the result of a fluid calculation with $\gamma = 0.16$ and $kT_e = 1$ eV, while ∗ denotes experimental data [44] obtained at $pL = 3.38$ Torr cm. (*b*) Spatial distribution of ion density obtained from the hybrid model using different values of γ, at $V = 400$ V. The cathode is situated at $x = 0$, while the anode is at $x = 3$ cm (also in all the forthcoming figures).

the modelling results at $\gamma = 0.16$ and the experimental curve can be explained by the radial losses of charged particles not being accounted for in the 1D model. Taking into account these losses in a 2D calculation a higher voltage would be required to sustain the same current, in this way moving the calculated $V–j/p^2$ curve towards the experimental one. (Preliminary results of a systematic comparison between 1D and 2D hybrid modelling have already been presented [44] and more detailed studies will be published in a forthcoming paper [45].)

The characteristic obtained from a fluid calculation is actually in quite good agreement with the measured $V–j/p^2$ curve, as shown in figure 1(*a*), while the characteristic calculated with the $\gamma = 0.3$ value (corresponding to a 'clean' cathode surface) strongly disagrees with the experimental result. Besides the $V–j/p^2$ curve the calculated density of the charged particles is also significantly influenced by the value of secondary yield, as illustrated in figure 1(*b*). At a constant voltage the calculated length of the cathode sheath decreases and the ion density in the negative glow increases with increasing γ.

While the voltage–current curve obtained from the fluid model fits relatively well the measured characteristic, it will be shown that, regarding other discharge characteristics, the results obtained based on the fluid approach strongly deviate from those obtained from the more accurate hybrid model. The spatial distributions of the electron and ion density obtained from the two types of models are compared in figure 2(*a*). For the same set of input parameters we can see more than two orders of magnitude difference between the peak values of the charge densities. The electric field distributions shown in figure 2(*b*) explain the difference of charge densities: while the hybrid model predicts a reversal of the sign of the electric field—this way building up a potential well where slow (bulk) electrons and ions can accumulate—the fluid model predicts $E > 0$ for the whole discharge gap (see especially the inset of figure 2(*b*)). This reversal of the electric field—caused by the strongly nonlocal ionization in the low-field negative glow— has attracted the interest of many authors [46,47] and is still a topic of recent studies [48,49].

The high gradient of the electric field profile plotted in figure 2(*b*) induces strongly nonequilibrium transport of the fast electrons. When, following their emission from the cathode, the electrons accelerate to an energy exceeding 50–60 eV, their total collision cross section is $\sigma \approx 10^{-16}$ cm^2. At 1 Torr pressure this results in a free path of $\lambda \approx 0.3$ cm. For these conditions $\lambda(\mathrm{d}E/\mathrm{d}x) \approx 200$ V cm^{-1} (see equation (8)), which is indeed comparable to the strength of the electric field itself. Under such conditions we would expect the electron distribution function to be very far from its equilibrium form at any position in the cathode sheath (cf section 2).

The calculations of the electrical characteristics shown in figure 1(*a*) have been carried out with constant values of γ which did not depend on discharge conditions. As a further improvement of the model one may consider the dependence of γ on discharge conditions, as will be illustrated below for the case of an abnormal argon glow discharge. The way to do this starts with identifying the dominant sources of electron emission from the cathode. For abnormal glow conditions positive ions and fast neutral atoms are found to be the particles mainly responsible for ejecting electrons from the cathode [14]. Provided that the energy-dependent secondary electron yields, $\gamma_i(\varepsilon)$ and $\gamma_a(\varepsilon)$, (probabilities that an electron is emitted from the cathode due to the impact of a positive ion or a fast atom) are known, the apparent yield can be self-consistently obtained from the simulation as [16,24]

$$\gamma = \frac{\sum_{k=1}^{N_i} \gamma_i(\varepsilon_k) + \sum_{k=1}^{N_a} \gamma_a(\varepsilon_k)}{N_i}, \qquad (9)$$

where N_i and N_a denote the number of ions and fast atoms arriving at the cathode due to the emission of N_0 primary electrons from the cathode and ε_k is the energy of the kth ion or atom.

Figure 3(*a*) displays electrical characteristics of Ar glow discharges obtained from a 1D hybrid calculation at $pL = 1$ Torr cm, by adopting different assumptions on the apparent secondary emission coefficient: (i) a constant value $\gamma = 0.06$ (often used in discharge models) and (ii) an apparent yield calculated according to (9). The additional curve labelled as 'H' also shown in figure 3(*a*) was obtained by using an apparent γ obtained for the case of *homogeneous* electric field
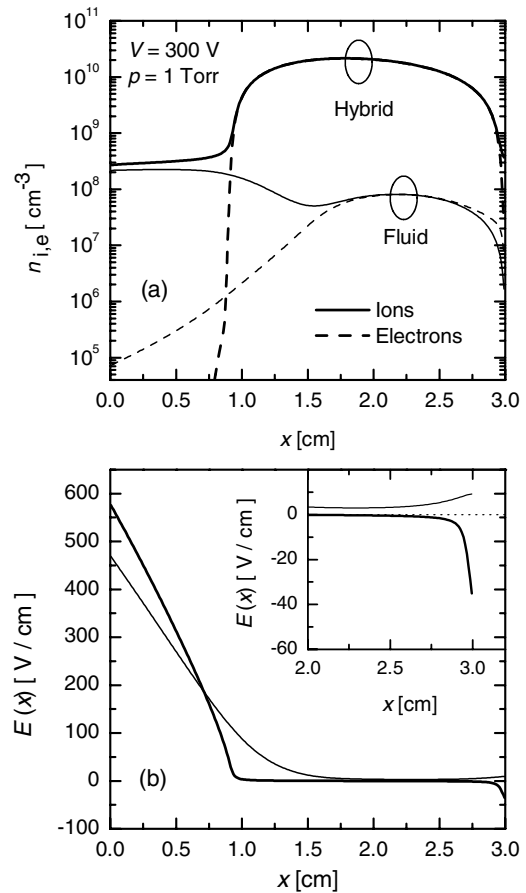

Figure 2. Comparison of the (*a*) charge density and (*b*) electric field distributions obtained from the fluid model (——) and from the hybrid model (——), at $p = 1$ Torr, $L = 3$ cm, $V = 300$ V and $kT_e = 0.3$ eV. The inset in (*b*) shows the low-field region near the anode.

(i.e. for a Townsend discharge) in [14]. It can immediately be seen, and should be kept in mind, that such data fail to be directly applicable to the simulation of discharges with well-developed cathode fall [15], as they predict physically incorrect electrical behaviour (a strong negative slope V–j/p^2 curve in the abnormal glow regime).

Figure 3(*b*) shows electrical characteristics obtained at different pL values, by using (9) in the modelling calculations. The results are in reasonable agreement with two sets of experimental data [50,51], which are also plotted in figure 3(*b*). The data of [50] were obtained using a 4.3 cm diameter copper cathode mounted on a six-way metal cross that itself served as the anode, while the data of [51] correspond to $pL = 0.5$ Torr cm experimental conditions in a discharge with plane-parallel electrodes.

Figure 3(*c*) shows the calculated dependence of the apparent electron yield (6) on the reduced electric field at the cathode. The data obtained through (9) can well be approximated as $\gamma = 0.01(E/n)_c^{0.6}$, independently of the value of pL, where $(E/n)_c$ is the reduced electric field at the cathode, given in units of kTds (1 kTd $= 10^{-20}$ V cm^2) [16]. The fact that γ changes a factor of three in the range of $(E/n)_c$ values covered (corresponding to 0.04 mA cm^{-2} Torr^{-2} $\leqslant$ $j/p^2 \leqslant 4$ mA cm^{-2} Torr^{-2}) shows that it would be more appropriate to calculate γ in discharge models rather than to
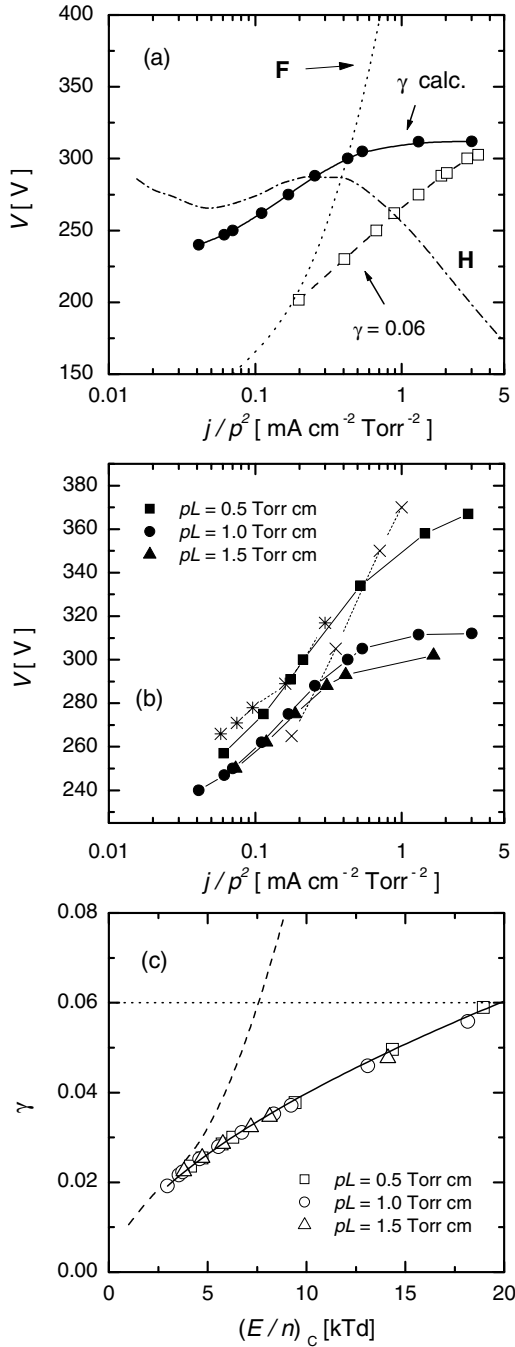
181

Figure 3. (*a*) Electrical characteristics of argon glow discharges obtained with different assumptions on the apparent electron yield: hybrid modelling results at $\gamma = 0.06$, γ calculated according to (9), H : assuming an electron yield obtained for homogeneous electric field in [14] and F : result of a fluid model with $\gamma = 0.06$. (*b*) Comparison of measured and calculated electrical characteristics (1D hybrid model using (9)). Experimental results: $\times$ [50], $*$ [51]. (*c*) Apparent electron yield calculated by (9) as a function of the reduced electric field at the cathode [16]. Dashed line: homogeneous field data [14], dotted line $\gamma = 0.06$ (1 kTd = 10^{-20} V cm^2).

use any constant value for it for a wide range of discharge conditions.

It is important to mention that as an alternative way one can consider the apparent γ as a fitting parameter and by adjusting its value one can match the calculated electrical characteristics
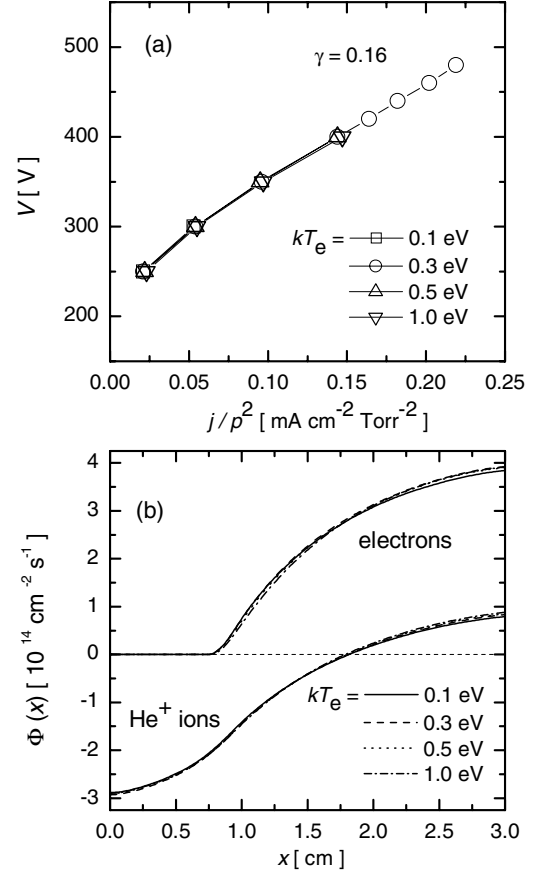

Figure 4. The effect of bulk electron temperature on the results of the simulations: (*a*) electrical characteristics and (*b*) fluxes of charged particles obtained with different values of kT_e, at $p = 1$ Torr helium, $L = 3$ cm, $V = 300$ V and $\gamma = 0.16$.

with their experimental counterparts [26, 27]. This way the possibility of the comparison between the calculated and experimental electrical characteristics is 'lost', but at least one can obtain information about the change of the self-sustainment mechanisms of the discharge with the varying conditions. This method usually yields γ values which vary with the operating conditions [52], in agreement with the findings of [14, 16].

Finally it is noted that secondary electron emission properties of the electrodes also influence the breakdown of RF discharges, as well as their operation in the 'gamma' regime [53].

3.2. Effect of bulk electron temperature

As mentioned in the introduction, hybrid models have routinely been using the bulk electron temperature kT_e as an input parameter, and in most of the papers $kT_e = 1$ eV is assumed. In order to analyse the effect on the calculated discharge characteristics of the bulk electron temperature we present the results of a series of hybrid simulations carried out with different values of kT_e.

Our simulations show that the electrical characteristics of the He glow discharge are not sensitive to the assumed value of kT_e, as indicated by the data plotted in figure 4(*a*). Similarly, the calculated fluxes of charged particles (which are strongly
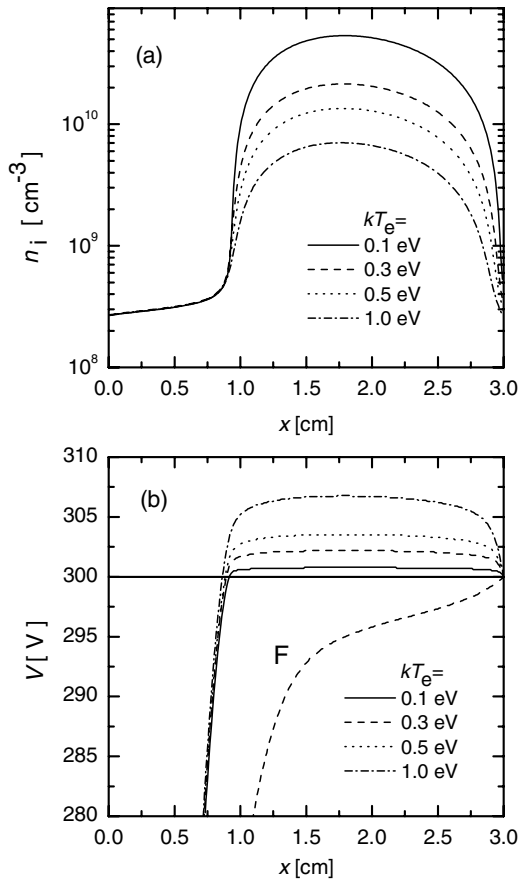
Figure 5. The effect of bulk electron temperature on the results of the simulations: (*a*) ion density distribution in the discharge gap and (*b*) spatial distribution of electric potential in the negative glow, at $p = 1$ Torr, $L = 3$ cm, $V = 300$ V, calculated at different values of kT_e. 'F': fluid calculation at $kT_e = 0.3$ eV.

connected to the electrical behaviour) are also not influenced to an observable extent by the choice of kT_e, see figure 4(*b*).

Another set of discharge characteristics, such as the charge density and the potential distribution in the negative glow, are, on the other hand, significantly influenced by the value of kT_e assumed in the model. This effect is illustrated in figure 5. For kT_e values decreasing from 1 to 0.1 eV we observe a steady and significant increase of the ion density (as well as of the electron density, which is not shown in the figure but is very nearly equal to the ion density in the glow region). Also, the plasma potential is influenced by the assumed value of kT_e: the potential well establishing in the negative glow gets deeper when kT_e is increased, as can be seen in figure 5(*b*).

It follows from the above findings that the electrical characteristics, charged particle fluxes and quantities related to these can be considered solid results of the hybrid modelling calculations that one can find in the literature. Concerning, however, details of the potential distribution and even more importantly charged particle densities, one should keep in mind that these calculated values have likely been influenced by the choice of the bulk electron temperature in the studies.

The reliability of the hybrid simulations could be improved (i) by using E/n-dependent transport coefficients in the calculations, (ii) by developing an accurate energy balance calculation for bulk electrons [6] or (iii) by using

experimentally determined values of kT_e. The first possibility, i.e. using $\mu_{e,i} = \mu_{e,i}(E/n)$ and $D_{e,i} = D_{e,i}(E/n)$, was found to result in numerical instabilities of the mathematical schemes used in hybrid models. There exist, on the other hand, different experimental techniques which can provide information about the bulk electron temperature. Using these techniques, previous experimental investigations on low pressure negative glow discharges usually resulted in cold electron temperatures significantly lower than 1 eV. These studies include laser based plasma diagnostics [54], Langmuir probe measurement [55–57], Thomson scattering measurements [58] as well as spectroscopic investigations of hollow cathode discharges [59]. In all these works cold electron temperatures ranging between 0.08 and 0.4 eV have been found. Considering these data, the 1 eV value, used in most hybrid model-based simulations, may be too high. Our probe measurements in helium glow discharges with plane-parallel electrodes [45] also confirm these lower ($\approx$0.1 eV) values of kT_e. The use of an accurate value for the bulk electron temperature may be even more important at higher gas pressures (and charge densities) when recombination processes—whose rates depend very strongly on T_e—become essential in the particle balance [31, 33].

4. Particle-in-cell approach

An alternative way of overcoming the problems of hybrid models associated with the temperature of the bulk electrons would be to use a fully kinetic simulation technique which would provide kT_e as a *result* instead of requiring its value as an input parameter. Thus we have tested the possibility of applying for a dc glow discharge the (electrostatic) *particle-in-cell* method complemented with the Monte Carlo description of collision processes (PIC/MCC), which has been used in studies of various types of plasmas, e.g. [60–65].

Since the details of the PIC/MCC method have been described in several papers, only the most important features are summarized here. Instead of treating all the particles of the plasma, the PIC method uses 'superparticles' which represent a (rather high) number of real particles. The number of superparticles used in the simulations is typically in the order of 10^4–10^5, although there exist larger scale simulations, as well. The superparticles are advanced in time by integrating their equations of motion under the effect of an electric field. The latter is found by solving on a spatial grid the Poisson equation, which takes into account as boundary condition the applied potential at the electrodes and the space charge density of the superparticles interpolated to a spatial grid. The interaction of the particles with electrode surfaces can easily be included in the simulations, as well as collision processes using the Monte Carlo technique.

In PIC models the point-like particles are replaced by charge clouds, of which the charges are distributed to at least two points of the computational grid (in 1D). This way the interaction of the closely separated electron–electron pairs is not considered precisely, only the long-range interaction of the charged particles is described correctly. The electron–electron (e–e) collisions can be incorporated into the PIC code using additional methods, e.g. [66]. The simulations presented here do not include e–e collisions.
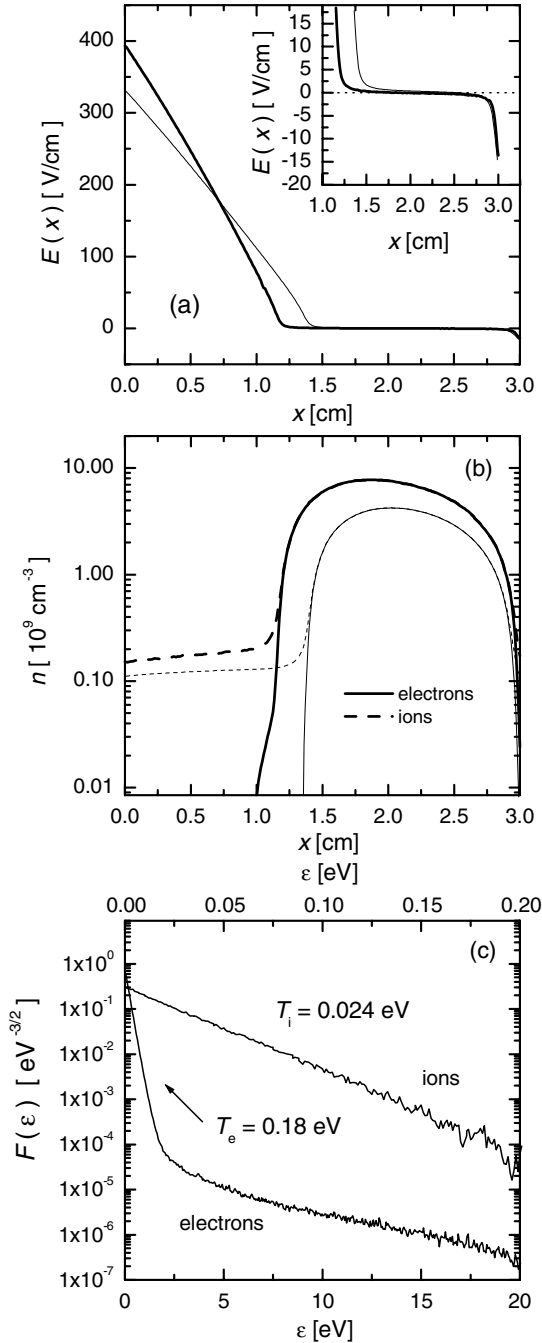
Figure 6. (*a*) Electric field distribution obtained from the PIC/MCC calculation at $V = 250$ V, $p = 1$ Torr, $L = 3$ cm and $\gamma = 0.15$ (——) and from a hybrid simulation assuming $T_e = 0.2$ eV and $\gamma = 0.16$ (——). The inset shows an enlarged part of the low-field negative glow region. (*b*) Charge densities from the PIC/MCC (——) and hybrid (——) simulations. (*c*) Electron (bottom scale) and ion (top scale) distribution functions at the position of the maximum of charge densities in the negative glow ($x \cong 1.9$ cm).

Our PIC/MCC code has been developed according to the well-known algorithms [60, 67]. Before testing the code for the dc case, first we have successfully cross-checked it with the benchmark results presented in [61] for 13.56 MHz helium discharges.

In the following, representative results obtained from testing the PIC/MCC simulation for a dc helium glow discharge

are presented. Figure 6 displays some of the calculated basic characteristics of a helium dc discharge operated at $V = 250$ V, $p = 1$ Torr and $L = 3$ cm with the secondary electron emission coefficient being set to $\gamma = 0.15$. Figure 6(*a*) displays the spatial distribution of the electric field. For comparison the result of a hybrid simulation—carried out with a similar set of input parameters and assuming $kT_e = 0.2$ eV—is also shown. $E(x)$ obtained from the PIC/MCC calculation exhibits the same qualitative features as its counterpart derived from the hybrid method. The high and linearly falling electric field strength in the cathode sheath is reproduced in both simulations. The reversal (sign change) of the electric field (and the negative value of the field at the anode) appears on both curves, as emphasized in the inset of figure 6(*a*). The spatial distributions of the electron and ion densities are plotted in figure 6(*b*). Again, the PIC/MCC and the hybrid simulations give similar results. The quantitative differences between the electric field and charge density distributions obtained from the two methods can be explained by the differences of the assumptions of the models, as well as the small differences of the sets of parameters used (values of γ and the different probabilities of the electron reflection from the anode).

The distribution functions of the electrons (EDF) and ions (IDF) are shown in figure 6(*c*), at the position in the negative glow where the charge densities are the highest. Linear fits to the graphs yield an ion temperature of $kT_i = 0.024$ eV and a bulk electron temperature of $kT_e = 0.18$ eV. $kT_i \cong kT_g = 0.026$ eV (where T_g corresponds to the gas temperature, 300 K) indicates that there is a thermal equilibrium between the ions and gas atoms in the negative glow. The value obtained for the electron temperature, $kT_e = 0.18$ eV, looks realistic and acceptable. The results shown here were obtained with a superparticle weight $W = 2 \times 10^5$ (resulting in $\approx 10^5$ superparticles), after simulating a time of about 2 ms. It is noted that in the case of PIC/MCC simulation of RF discharges in most studies ≈ 1000 RF cycles are simulated, which, for $f = 13.56$ MHz frequency, correspond to ≈ 74 μs. Convergence of the results in the dc case was reached in about 30 times longer time.

In view of the results presented in figure 6 one may be convinced that the PIC/MCC method is able to correctly describe the dc glow considered here. However, when testing the simulation with different values of the superparticle weight W we observe a significant sensitivity of the bulk electron temperature and charge density in the negative glow to W. This effect is illustrated in figures 7(*a*) and (*b*), where the charge densities and the EDF, respectively, are plotted for different values of W. A change of W by a factor of eight results in a change of peak charge densities by a factor of three—$n_{i,max}$ increases with decreasing W (i.e. with an increasing number of superparticles). The opposite effect of W on kT_e is also clearly visible.

Although the application of the PIC/MCC technique for the dc abnormal glow discharges clearly failed, it brought attention to the importance of testing the simulation parameters, first of all the number of superparticles used in the calculations. Such a test may also be advisable in the case of RF discharge simulations, as in some of the earlier studies dependence of the results on the number of superparticles has indeed been reported, see e.g. [68]. We believe that the
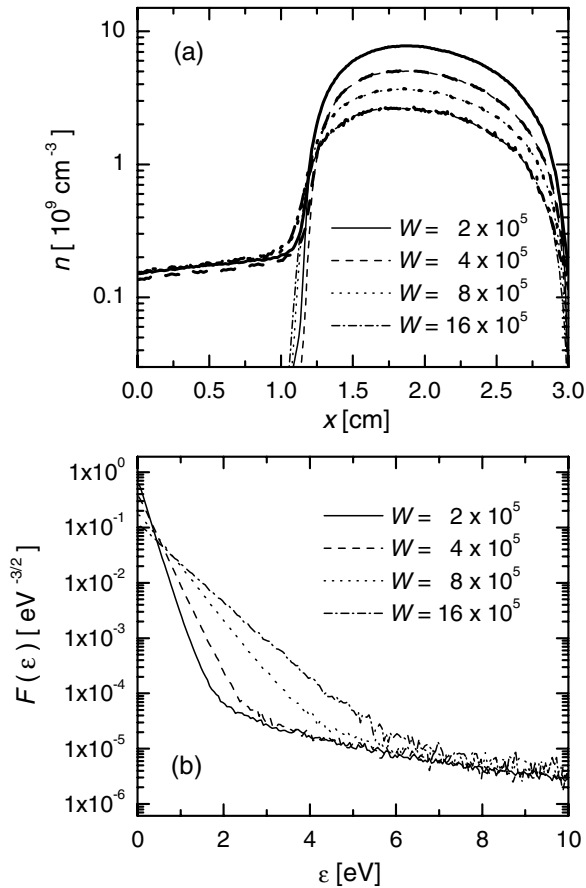
Figure 7. (*a*) Charge density distributions and (*b*) electron distribution functions at ($x \cong 1.9\,\mathrm{cm}$) obtained from the PIC/MCC calculation at $V = 250\,\mathrm{V}$, $p = 1\,\mathrm{Torr}$, $L = 3\,\mathrm{cm}$ and $\gamma = 0.15$, using different values of the superparticle weight W.

problems of the PIC/MCC method found here are associated with the long trapping time of bulk electrons, vastly exceeding the numerical relaxation time of the simulation arising from spurious numerical effects. A more detailed explanation of the above observations and limitations of the PIC/MCC technique in general is to be published [69].

5. Conclusions

In conclusion, hybrid models can be safely said to represent today's most reliable class of models for the description of dc glow discharges, due to their flexibility and reliability regarding the determination of some of the calculated discharge characteristics. Their limitations, e.g. in the prediction of absolute values of charge densities, should, however, be kept in mind. As these uncertainties originate from inadequate knowledge of the bulk electron temperature, by complementing the simulations with experimental determination of the electron temperature, the reliability of the hybrid models can be improved. Additionally, extensive data for electron yields of cathode materials under discharge conditions would be needed for more reliable results. One should bear in mind that neither (i) electron yield values obtained from ion beam bombardment of heavily sputtered samples under ultrahigh vacuum conditions nor (ii) electron

yield values derived from Townsend discharge experiments can directly be applied in simulations of abnormal glow discharges. In the former case the cathode surface conditions are different from those found in typical discharge chambers, while in the latter case the different electric field distribution results in a dissimilar energy distribution of species bombarding the cathode thereby modifying the apparent electron yield.

The study of the applicability of the PIC/MCC approach for the description of (strongly collisional) dc abnormal glow discharges pointed out the need for checking the simulation results (which, at first sight, may even look realistic). Checking the sensitivity of the modelling results to the number of superparticles used in PIC/MCC simulations is advisable in general, including studies of RF discharges.

The continuous increase in computing speed raises hope for fully kinetic simulations of abnormal dc glow discharges, provided that reliable techniques can be found. As an important alternative technique to particle simulations, the solution of the Boltzmann equation may be mentioned. During recent years one could witness the dramatic progress of applications of the Boltzmann equation for practical discharge problems, see e.g. [70, 71]. Spatially varying electric fields can be routinely handled in the solution schemes developed. Considering the use of Boltzmann equation-based techniques for self-consistent studies of the cathode region of dc glow discharges, the peculiar effect of the electric field reversal in the negative glow region may be recognized as the main difficulty. A complete solution of the problems associated with the reversal of the electric field is the subject of current efforts [72].

Acknowledgments

References

[1] Surendra M, Graves D B and Jellum G M 1990 *Phys. Rev.* A **41** 1112
[2] Boeuf J-P and Pitchford L C 1991 *IEEE Trans. Plasma Sci.* **19** 286
[3] Dalvie M, Hamaguchi S and Farouki R T 1992 *Phys. Rev.* A **46** 1066
[4] Phelps A V, Petrović Z Lj and Jelenković B M 1993 *Phys. Rev.* E **47** 2825
[5] Bogaerts A, Gijbels R and Goedheer W J 1996 *Anal. Chem.* **68** 2296
[6] Arslanbekov R R, Kudryavtsev A A 1998 *Phys. Rev.* E **58** 6539
[7] Shidoji E, Ohtake H, Nakano N, Makabe T 1999 *Japan. J. Appl. Phys.* **38** 2131
[8] Arslanbekov R R and Kolobov V I 2003 *J. Phys. D: Appl. Phys.* **36** 2986
[9] Sukhinin G I and Fedoseev A V 2003 *Plasma Phys. Rep.* **29** 1062
[10] Goedheer W J, Akdim M R and Chutov Yu I 2004 *Contrib. Plasma Phys.* **44** 395
[11] Robson R E, White R D and Petrović Z Lj 2005 *Rev. Mod. Phys.* **77** 1303

[12] Phelps A V 2001 *Plasma Sources Sci. Technol.* **10** 329
[13] Auday G, Guillot P, Galy J and Brunet H 1998 *J. Appl. Phys.* **83** 5917
[14] Phelps A V and Petrović Z Lj 1999 *Plasma Sources Sci. Technol.* **8** R21
[15] Phelps A V, Pitchford L C, Pedoussat C C and Donkó Z 1999 *Plasma Sources Sci. Technol.* **8** B1
[16] Donkó Z 2001 *Phys. Rev.* E **64** 026401
[17] Bogaerts A and Gijbels R 2002 *Plasma Sources Sci. Technol.* **11** 27
[18] Malović G, Strinić A, Živanov S, Marić D and Petrović Z Lj 2003 *Plasma Sources Sci. Technol.* **12** S1
[19] Marotti D, McLaughlin J A and Maguire P 2004 *Plasma Sources Sci. Technol.* **13** 207
[20] Sosov Y and Theodosiou C E 2004 *J. Appl. Phys.* **95** 4385
[21] Raizer Y P, Ebert U and Sijacic D D 2004 *Phys. Rev.* E **70** 017401
[22] Bokhan A P, Bokhan P A and Zakrevsky D E 2005 *Appl. Phys. Lett.* **86** 151503
[23] Revel I, Pitchford L C and Bouef J-P 2000 *J. Appl. Phys.* **88** 2234
[24] Donkó Z 2000 *J. Appl. Phys.* **88** 2226
[25] Bogaerts A and Gijbels R 1997 *Spectrochim. Acta* B **52** 765
[26] Marić D, Hartmann P, Malović G, Donkó Z and Petrović Z Lj 2003 *J. Phys. D: Appl. Phys.* **36** 2639
[27] Kutasi K and Donkó Z 2000 *J. Phys. D: Appl. Phys.* **33** 1081
[28] Callegari Th, Ganter R and Boeuf J-P 2000 *J. Appl. Phys.* **88** 3905
[29] Bogaerts A and Gijbels R 1998 *Spectrochim. Acta* B **53** 437
[30] Boeuf J-P and Garrigues L 1998 *J. Appl. Phys.* **84** 3541
[31] Kutasi K, Hartmann P and Donkó Z 2001 *J. Phys. D: Appl. Phys.* **34** 3368
[32] Bogaerts A and Gijbels R 1999 *J. Appl. Phys.* **86** 4124
[33] Kutasi K, Hartmann P, Bánó G and Donkó Z 2005 *Plasma Sources Sci. Technol.* **14** S1
[34] Bogaerts A, Gijbels R and Carman R J 1998 *Spectrochim. Acta* B **53** 1679
[35] Peres I, Pitchford L C 1995 *J. Appl. Phys.* **78** 774
[36] Bogaerts A, Gijbels R 1999 *Plasma Sources Sci. Technol.* **8** 210
[37] Hartmann P, Matsuo H, Ohtsuka Y, Fukao M, Kando M and Donkó Z 2003 *Japan. J. Appl. Phys.* **42** 3633
[38] Donkó Z 1998 *Phys. Rev.* E **57** 7126
[39] Nienhuis G J, Goedheer W J, Hamers E A G, van Sark W G J H M and Bezemer J 1997 *J. Appl. Phys.* **82** 2060
[40] Brok W J M, van Dijk J, Bowden M D, van der Mullen J J A M and Kroesen G M W 2003 *J. Phys. D: Appl. Phys.* **36** 1967
[41] Kim H C, Iza F, Yang S S, Radmilović-Radjenović M and Lee J K 2005 *J. Phys. D: Appl. Phys.* **38** R283
[42] Hagelaar G J M and Pitchford L C 2005 *Plasma Sources Sci. Technol.* **14** 722
[43] Hayden H C and Utterback N G 1964 *Phys. Rev.* **135** A1575
[44] Hartmann P, Kutasi K and Donkó Z 2005 Comparison of one- and two-dimensional hybrid modeling of low-pressure gas discharges *Proc. 27th ICPIG (Eindhoven, The Netherlands, July 17–22, 2005)* contribution 03-262
[45] Hartmann P, Kutasi K, Bánó G, Donkó Z 2006 in preparation
[46] Gottscho R A, Mitchell A, Scheller G R, Chan Y and Graves D B 1989 *Phys. Rev.* A **40** 6407
[47] Bouef J-P and Pitchford L C 1995 *J. Phys. D: Appl. Phys.* **28** 2083
[48] Pinheiro M 2004 *Phys. Rev.* E **70** 056409
[49] Kudryavtsev A A and Toinova N E 2005 *Tech. Phys. Lett.* **31** 370
[50] Rózsa K, Gallagher A and Donkó Z 1995 *Phys. Rev.* E **52** 913
[51] Stefanović I and Petrović Z Lj 1997 *Japan. J. Appl. Phys.* **36** 4728
[52] Marić D, Kutasi K, Malović G, Donkó and Petrović Z Lj 2002 *Eur. Phys. J.* D **21** 73
[53] Radmilović-Radjenović M and Lee J K 2005 *Phys. Plasmas* **12** 063501
[54] Den Hartog E A, O'Brian T R and Lawler J E 1989 *Phys. Rev. Lett.* **62** 1500
[55] Bogaerts A, Quentmeier A, Jakubowski N and Gijbels R 1995 *Spectrochim. Acta* B **50** 1337
[56] Angstadt A D, Whelan J and Hess K R 1993 *Microchem. J.* **47** 206
[57] Ohsawa A, Ohuchi M and Kubota T 1991 *Meas. Sci. Technol.* **2** 801
[58] Gamez G, Bogaerts A, Andrade F and Hieftje G 2004 *Spectrochim. Acta* B **59** 435
[59] Bánó G, Szalai L, Horváth P, Kutasi K, Donkó Z, Rózsa K and Adamowicz T M 2002 *J. Appl. Phys.* **92** 6372
[60] Birdsall C K 1991 *IEEE Trans. Plasma Sci.* **19** 65
[61] Surendra M 1995 *Plasma Sources Sci. Technol.* **4** 56
[62] Vender D and Boswell R W 1990 *IEEE Trans. Plasma Sci.* **18** 725
[63] Taccogna F, Longo S and Capitelli M 2003 *Eur. Phys. J. Appl. Phys.* **22** 29
[64] Georgieva V, Bogaerts A and Gijbels R 2004 *Phys. Rev.* E **69** 026406
[65] Meige A, Boswell R, Charles C and Turner M 2005 *Phys. Plasmas* **12** 052317
[66] Nanbu K 1997 *Phys. Rev.* E **55** 4642
[67] Nanbu K 2000 *IEEE Trans. Plasma Sci.* **28** 971
[68] Schweigert I V, Scheweigert V A 2004 *Plasma Sources Sci. Technol.* **13** 315
[69] Turner M M 2006 Kinetic properties of particle-in-cell simulations compromised by Monte Carlo collisions submitted
[70] Sigeneger F, Winkler R 2002 *Eur. Phys. J. Appl. Phys.* **19** 211
[71] Winkler R, Arndt S, Loffhagen D, Sigeneger F and Uhrlandt D 2004 *Contrib. Plasma Phys.* **44** 437
[72] Loffhagen D, Sigeneger F and Winkler R 2004 *Eur. Phys. J. Appl. Phys.* **25** 45